Development and validation of a sensor prototype for near-infrared imaging of the newborn brain

Ahnen, Linda ; Stachel, Helene ; Kleiser, Stefan ; Hagmann, Cornelia ; Jiang, Jingjing ; Kalyanov, Alexander ; Lindner, Scott ; Wolf, Martin ; Sanchez, Salvador

Abstract: Imaging brain oxygenation is crucial for preventing brain lesions in preterm infants. Our aim is to build and validate a near-infrared optical tomography (NIROT) sensor for the head of neonates. This sensor, combined with an optoacoustic device, will enable quantitative monitoring of the structural and functional information of the brain. Since the head of preterm infants is small and fragile great care must be taken to produce a comfortable and compact device in which a sufficient number of light sources and detectors can be implemented. Here we demonstrate our first prototype. Heterogeneous silicone phantoms were produced to validate the prototype's data acquisition, data processing, and image reconstruction. Reconstructed optical properties agree well with the target values. The mechanical performance of the new NIROT sensor prototype confirms its suitability for the clinical application.

DOI: https://doi.org/10.1007/978-3-319-55231-6_22

Development and Validation of a Sensor Prototype for Near-Infrared Imaging of the Newborn Brain

Linda Ahnen, Helene Stachel, Stefan Kleiser, Cornelia Hagmann, Jingjing Jiang, Alexander Kalyanov, Scott Lindner, Martin Wolf and Salvador Sanchez

Biomedical Optics Research Laboratory, University Hospital Zurich, Switzerland

Abstract Imaging brain oxygenation is crucial for preventing brain lesions in preterm infants. Our aim is to build and validate a near-infrared optical tomography (NIROT) sensor for the head of neonates. This sensor, combined with an optoacoustic device, will enable quantitative monitoring of the structural and functional information of the brain. Since the head of preterm infants is small and fragile great care must be taken to produce a comfortable and compact device in which a sufficient number of light sources and detectors can be implemented. Here we demonstrate our first prototype. Heterogeneous silicone phantoms were produced to validate the prototype's data acquisition, data processing, and image reconstruction. Reconstructed optical properties agree well with the target values. The mechanical performance of the new NIROT sensor prototype confirms its suitability for the clinical application.

1 Introduction

Cerebral ischemia is one of the key initiating factors for white matter injuries and intraventricular hemorrhage in preterm infants [1]. These pathologies are associated with long-term neurodevelopmental impairments. We are in the design process of a novel multimodal hybrid diagnostic imager to quantitatively monitor brain oxygenation. The novel imager will integrate an optoacoustic (OA) [2] device and a near-infrared optical tomography (NIROT) [3] sensor in a single system. The OA device includes an US transducer, which obtains structural information of the brain. NIROT will image a more diffuse 3D map of the oxygenation of the preterm baby's brain. Additionally, NIROT provides a 3D fluence (light intensity) estimation of the OA source, which can then be used to obtain quantitative oxygena-

tion values in the OA image. In order to design the prototype NIROT sensor, geometric constraints and medical conditions have to be considered.

For accurate reconstructions of the optical properties in the region of interest, a sufficient number of light sources and detectors need to be implemented. The average head circumference of prematurely born infants varies between 21 cm and 35 cm for gestational age ranging fom 23 to 41 weeks [4]. This severely limits the space available for NIROT measurements. Further spatial constraints result from the combination with the OA probe that necessarily uses the fontanel aperture for measurements. In order to obtain good quality signals, no light may pass directly between source and detector fibers. Also, the knowledge of the location of the source and detector fibers is crucial for a precise 3D image reconstruction [5]. Additionally, the head's irregular geometry poses difficulties for a good coupling of the light fibers to the skin. The fragile skin of premature infants has to be protected from any injuries. Additionally, sensor materials have to be biocompatible and need to be easy to clean and disinfect. Our aim is to build a prototype NIROT sensor that fulfils these requirements and is suitable for clinical application.

2 Methods

2.1 NIROT Sensor Overview

The NIROT sensor geometry is a ring structure, leaving space in its center for the OA device, which consists of a handheld ultrasound probe and a light source. The NIROT sensor includes 16 source and 4 detector microfiber bundles (Loptek GmbH & Co. KG, Berlin, Germany), fixed to a rigid ring (diameter 4.6 cm), which is embedded into soft silicone. The source and detector microfibers bundles consist of about 470 and 570 microfibers, with a diameter of 30 µm and 70 µm, respectively. The source and detector bundles have a bending radius of 4 mm and 7 mm, respectively. They are highly flexible and thus provide space for the OA device. Measurements are performed using the commercially available Imagent (ISS Inc., Champaign, IL, USA). It consists of 2x16 laser diodes that emit near-infrared light at 760 nm and 834 nm with an output power of 10 mW. Four photomultiplier tubes serve as light detectors. The Imagent is a frequency domain (110 MHz) near-infrared spectroscopy device, which measures the phase, amplitude, and mean of the sinusoidally modulated light intensity.

2.2 Development of NIROT Sensor

In a first step, the light fibers are inserted into the 3D printed rigid ring (Fig. 1a, ring in dark grey) and fixed with M 1.2 screws (Fig. 2a). This ensures a fixed relative position of the sensor's source and detector fibers during the measurement. This ring, together with the fibers, is then placed into the mold (Fig. 1a) to cast a black silicone casing (Fig. 2b).
The inner ring and the mold of the NIROT sensor are produced using an Ultimaker 2 (Ultimaker B.V., Geldermalsen, the Netherlands) fused deposition modelling 3D printer. Acrylonitrile butadiene styrene (ABS) is heated up and deposited in small layers following the computer model of the different parts (Fig. 1). The nozzle size was 0.4 mm. For the 3D prints a layer height of 0.07 mm, a shell thickness of 1.4 mm, a fill density of 35% and a print speed of 50 mm/s is chosen. The outer shell printing speed is reduced to 35 mm/s to ensure an accurate printing. All 3D printed parts are sandpapered thoroughly to remove any directionality of the printing material. This is important to avoid any surface structures in the silicone, which might cause light piping. The black silicone casing surrounds the entire ring-fiber structure with silicone, except the fiber ends (Fig 2b). This prevents light piping from source to detector fibers. In a second casting step, the mold shown in Fig. 1b and 1c was employed to fill transparent silicone into the hollow space around the fiber ends to create optical windows. To ensure a good light coupling into tissue, the optical windows were designed to be slightly elevated from the black silicone structure as can be seen in Figure 1b (part 4). The soft silicone casing (Silpuran 2400/25 and Elastosil black RAL9011, WACKER Silicones, Burghausen, Nünchritz, Germany) is biocompatible and easy to disinfect. It allows the sensor to slightly adapt to the geometry of the head and prevents skin lesions. The finished NIROT sensor is shown in Fig. 3. In the NIROT sensor ring, the source-detector distance covers a range from 0.7 cm up to 4.6 cm. This results in a light intensity variation in the order of 10^3 [6], which exceeds the Imagent dynamic range. In order to address this problem, the emitted light intensity is attenuated with neutral density filters of varying optical density. The optical density of the filters is inversely correlated with source and detector distance to maintain an approximately constant light intensity at the detectors for a homogeneous medium.

2.3 Validation with Phantoms

Two heterogeneous silicone head phantoms with optical properties similar to the target application in preterm infants [7] were produced to validate the NIROT sensor (Fig. 3b). For this a 3D surface structure was extracted from MRI data and printed. From this 3D printed head a silicone mold was made to produce realistic head phantoms. Differently sized inclusions may be inserted into the head phan-

tom's silicone mold. Here, spherical inclusions were employed to simulate localized lesions in the brain with a step change in optical properties. The head circumference of the phantoms was 28 cm. The phantoms consisted of a bulk material with an absorption coefficient of $\mu_a \approx 0.005$ mm^{-1} and a reduced scattering coefficient of $\mu_s' \approx 0.5$ mm^{-1}. The spherical inclusions (diameter 1.5 cm) in the head phantom were chosen to have larger absorption than the bulk material ($\mu_a \approx 0.05$ mm^{-1} and $\mu_a \approx 0.02$ mm^{-1}). The μ_s' of the inclusions was the same as the background. Image reconstructions of optical properties were performed with the software Nirfast [8, 9] based on data measured with the Imagent. Nirfast is a finite element software to simulate light propagation in tissue. For the reconstruction, a spherical shape was implemented in Nirfast to model the phantom head. During the 3D image reconstruction μ_s' was assumed to be constant.

3 Results, Discussion and Conclusion

The new NIROT sensor prototype is compact and light. The ease of handling makes it very suitable for the clinical application at the bedside, where space is limited. The elevated optical windows of the sensor enable moderate adaption to the head's surface, ensuring good light coupling. No light piping between the source and detector fibers was detected during the measurements on the silicone head phantoms. Figure 4 shows two center cross-sections of the 3D reconstructed image for the phantom with the spherical inclusion with $\mu_a \approx 0.05$ mm^{-1}. The shape and location of the inclusion was accurately reconstructed. Although the reconstruction model assumes a spherical head shape, it is applied onto a non-spherical head phantom. This results in a slight distortion of the inclusion shape as is visible in Fig. 4. The reconstructed μ_a of the spherical inclusions are lower than the target values (see Section 2.3). This is a well-known effect and mainly results from the smearing of the original spherical inclusion.

Here, we have presented a first prototype NIROT sensor that fulfils all the requirements for its clinical application (together with the OA device). The sensor has been validated with phantoms and in the near future the NIROT sensor will be tested in a dedicated clinical trial. For this the NIROT sensor design will be slightly changed to fit an egg-like shape, corresponding closer to the head than the current spherical shape to enable measurements in patients.

Acknowledgments This work was supported by the SwissTransMed project ONIRIUS, Swiss Cancer Research project KFS-3732-08-2015, KFSP Tumor Oxygenation and KFSP Molecular Imaging Network Zurich of the University Zurich, Swiss National Science Foundation (Grant number 139238 and 159490) and by the National Competence Center for Biomedical Imaging.

References

1. O. Khwaja, J. J. Volpe (2008). Pathogenesis of cerebral white matter injury of prematurity. Archives of Disease in Childhood-Fetal and Neonatal Edition, 93(2), F153-F161.
2. P. Beard (2011). Biomedical photoacoustic imaging. Interface focus, rsfs20110028.
3. J. C. Hebden, T. Austin (2007). Optical tomography of the neonatal brain. European radiology, 17(11), 2926-2933.
4. A. Barbier, A. Boivin, W. Yoon, et al (2013). New Reference Curves for Head Circumference at Birth, by Gastational Age. Pediatrics 131(4),e1158 doi: 10.1542peds.2011-3846
5. L. Ahnen, M. Wolf, C. Hagmann, et al (2016). Near-Infrared Image Reconstruction of Newborns' Brains: Robustness to Perturbations of the Source/Detector Location. In Oxygen Transport to Tissue XXXVII (pp. 377-382). Springer New York.
6. D. M. Hueber, S. Fantini, A. E. Cerussi, et al (1999, July). New optical probe designs for absolute (self-calibrating) NIR tissue hemoglobin measurements. In BiOS'99 International Biomedical Optics Symposium (pp. 618-631). International Society for Optics and Photonics.
7. Arri, S. J., Muehlemann, T., Biallas et al (2011). Precision of cerebral oxygenation and hemoglobin concentration measurements in neonates measured by near-infrared spectroscopy. Journal of biomedical optics, 16(4), 047005-047005.
8. M. Jermyn, H. Ghadyani, M.A. Mastanduno et al (2013) Fast segmentation and high-quality three-dimensional volume mesh creation from medical images for diffuse optical tomography. J. Biomed. Opt. 18 (8), 086007 doi: 10.1117/1.JBO.18.8.086007.
9. H. Dehghani, M.E. Eames, P.K. Yalavarthy et al (2009) Near infrared optical tomography using NIRFAST: Algorithm for numerical model and image reconstruction. Communications in Numerical Methods in Engineering, vol. 25, 711-732.

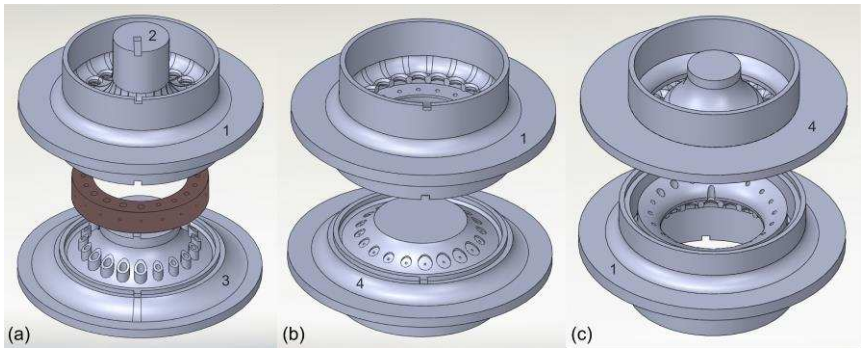

Fig. 1. (a) shows the mold employed to cast the black silicone casing. It consists of parts 1, 2, and 3. The rigid ring to which the fibers will be fixed is shown in dark grey. (b) and (c) show two views of the mold (parts 1 and 4) used to fill the optical windows with transparent silicone.

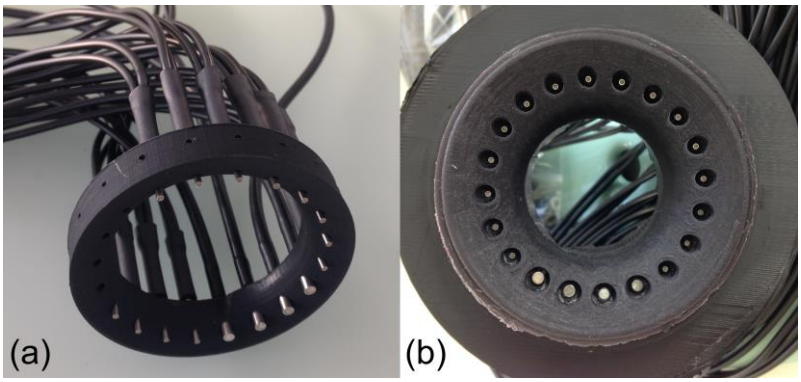

Fig. 2. (a) shows the 3D printed rigid inner ring. Some source and detector fibers are fixed to it with the help of screws that are inserted perpendicular to the fibers. (b) shows the fiber/ring structure embedded into black biocompatible silicone casing. The space around the fiber ends will later be filled with transparent silicone in order to create optical windows.

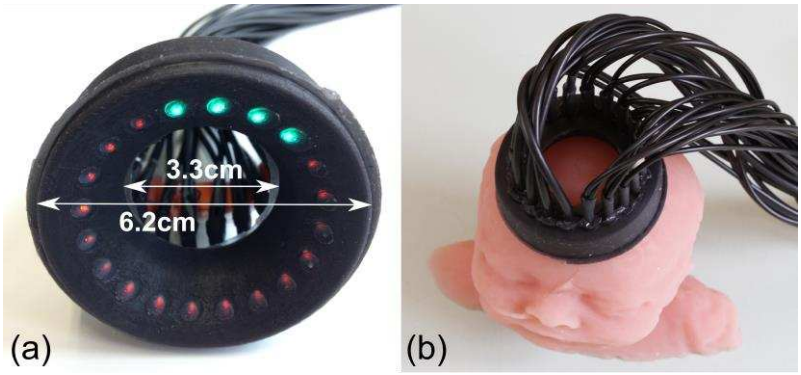

Fig. 3. (a) Finished NIROT sensor prototype with 16 sources and 4 detectors. (b) shows the NIROT sensor placed on a silicone baby head phantom. The fibers are spread apart to provide space in the middle for the OA measurement.

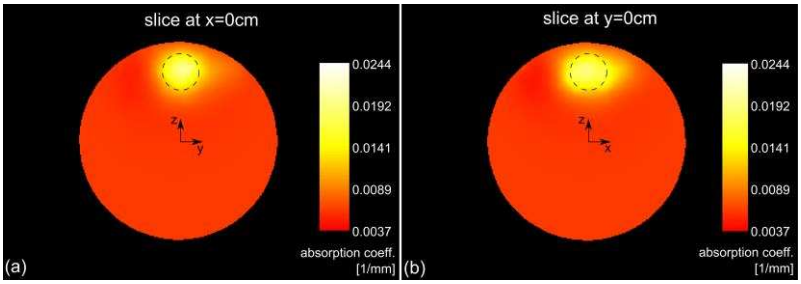

Fig. 4. Two center cross-sections of the 3D image reconstruction of the absorption coefficient are shown. The bulk absorption coefficient is $0.005mm^{-1}$ and $0.05mm^{-1}$ of the spherical inclusion. The spherical inclusion's actual size and location is shown in dashed lines.